Real-Time Observation and Analysis of Magnetomechanical Actuation of Magnetic Nanoparticles in Cells

Arnaud Hillion, Nicolas Hallali, Pascal Clerc, Sara Lopez, Yoann Lalatonne, Camille Noûs, Laurence Motte, Véronique Gigoux, Julian Carrey

Real-time observation and analysis of magneto-mechanical actuation of magnetic nanoparticles in cells

A. Hillion[1#], N. Hallali[1#], P. Clerc[1,2#], S. Lopez[1,2], Y. Lalatonne[3], C. Noûs[4], L. Motte[3*#], V. Gigoux[1,2*#], J. Carrey[1*#].

[1] Laboratoire de Physique et Chimie des Nano-Objets, CNRS UMR5215-INSA, Université de Toulouse III, Toulouse, France.

[2] INSERM ERL1226, Receptology and Targeted Therapy of Cancers, Toulouse, France.

[3] Université Sorbonne Paris Nord and Université de Paris, INSERM, LVTS, F-75018 Paris, France.

[4] Laboratoire Cogitamus, Université de Toulouse III, Toulouse, France.

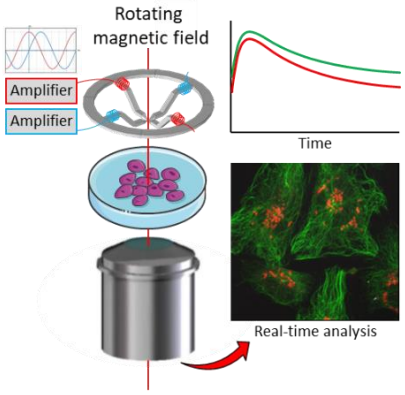

ABSTRACT: The origin of cell death in the magneto-mechanical actuation of cells induced by magnetic nanoparticles motion under low frequency magnetic fields is still elusive. Here, a miniaturized electromagnet fitting under a confocal microscope is used to observe in real-time cells specifically targeted by superparamagnetic nanoparticles and exposed to a low frequency rotating magnetic field. Our analysis reveals that the lysosome membrane is permeabilized a few minutes only after the start of magnetic field application, concomitantly with lysosomes movements towards the nucleus. Those events are associated with the tubulin microtubules network disorganization and change in cell morphology. This miniaturized electromagnet will permit to get a deeper insight into the physical, molecular, and biological process occurring during the magneto-mechanical actuation of magnetic nanoparticles.

KEYWORDS: Magnetic nanoparticles, rotating low frequency magnetic field, mechanical forces, lysosome, microtubules.

The magnetic properties of nanoparticles make them ideal for using in various applications, especially biomedical ones. In the last decades, they have been used in domains such as bioimaging, magnetic manipulation, enzyme-like activity, magnetic hyperthermia and responsive drug delivery [1–10]. Recently, a new field has attracted attention: the cancer treatment *via* magneto-mechanical actuation of cell death [11–16], which is based on the energy conversion of external low frequency magnetic field into mechanical forces by magnetic nanoparticles (MNPs) [17]. Low-frequency magnetic fields are technically less challenging to be generated at the human scale and display less adverse effects than the high frequency ones used in magnetic hyperthermia. Such treatment requires the loading of cells membranes or organelles such as lysosomes with MNPs and the subsequent application of external magnetic fields. Recent literature shows that the mechanical forces exerted by MNPs, accumulated in lysosomes, under alternating or rotating magnetic field treatment are large enough to disrupt lysosomal membranes, resulting in lysosome membrane permeabilization and the subsequent initiation of cell death. For instance, Zhang *et al.* [18] demonstrated the induction of lysosome permeabilization after applying a rotating 30 mT field at 20 Hz for 20 min with MNPs targeting lysosomes. Shen *et al.*[19] dramatically damaged the plasma and lysosomal membranes under a low-frequency rotating magnetic field at 15 Hz and 40 mT, on cells exposed to zinc-doped iron oxide nanoparticles. Lunov *et al.* [20] revealed that MNPs retained in lysosomal compartments can be effectively actuated with a pulsed magnetic field, resulting in LMP in cancer cells. Two studies showed cells with a disorganized actin cytoskeleton following the pulsed AC low frequency magnetic field application (62 mT / 50 Hz) or a low-frequency rotating magnetic field at 15 Hz and 40 mT, but without quantifying precisely this disorganization [21, 15]. In all the experiments reported so far, magnetic fields were first applied on cancer cells and the resulting effects observed subsequently. In the present article, we describe a successful approach to achieve real-time cell imaging during the magnetic field exposure, based on a setup able to apply a localized low frequency rotating magnetic field (RMF) under a confocal microscope. This setup permits to establish the precise timetable of the specific mechanisms or biological effects induced by the magnetic field application such as lysosome permeabilization and motility as well as microtubules network disorganization or change in cell morphology.

The MNPs (USPION@Gastrin) used here for magneto-mechanical cell destruction are composed of an ultra-small iron oxide nanoparticle with 6-nm core diameter, coated with PEG-COOH, and decorated with a fluorophore (DY647) and a synthetic replicate of gastrin. The later binds specifically to the cholecystokinin-2 (CCK2) receptor – a receptor expressed in different cancers including the pancreatic cancer – and allows the specific MNPs internalization in cells expressing this receptor. We showed that USPION@Gastrin are embeded in lysosomal vesicles following 24h of incubation (see Supplemental Information, Figure S1 and Ref. [22]). Then, the application of a 40 mT / 1 Hz RMF (magnetic field parameters inducing the highest rate of cell death) disrupt 34% of CAFs cells having accumulated USPION@gastrin within their lysosomes [22]. To study the effect in real-time of RMF treatment, an electromagnet consisting in four identical coils containing soft iron cores was placed in the Cellview dish containing cells having or not internalized MNPs, under a confocal microscope (Figure 1 and Supplemental Information, Figure S2). The electromagnet was gold-plated to ensure its biocompatibility. The application of a sinusoidal current with a 90° phase shift between two pairs of opposite coils creates a rotating magnetic field between the four tips of soft iron. The zone between the tips measures approximately 1 mm^2. In all experiments described thereafter, a 40 mT / 1 Hz RMF was used, since we show previously that these are the conditions maximizing cell death (34% of CAF cells disrupted) [23]. The temperature of the cell incubation medium was monitored and is maintained around 37°C during RMF experiment (Supplemental Information, Figure S3).

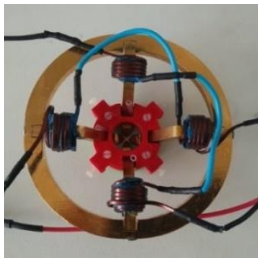

Figure 1. Picture of the miniaturized electromagnet.

We first traced the lysosome permeabilization during magnetic field exposure by measuring the Lysotracker release from lysosomes. Confocal images of cells containing MNPs and exposed or not to RMF are shown in the Figure 2a, where the Lysotracker is in green, the USPION@Gastrin in red, and the USPION@Gastrin/Lysotraker colocalization in yellow. In this representative image, a drop of Lysotracker fluorescence intensity in cells exposed to RMF comparatively to control cells (RMF-) is observed. The spatial colocalization between the two fluorescent species was analyzed through the calculation of Pearson's correlation coefficient (Figure 2b). At t0, the Pearson's correlation coefficient values are respectively 0.76 ± 0.05 and 0.71 ± 0.02 in the absence (USPION@Gastrin) or in the presence of RMF application (USPION@Gastrin + RMF), confirming the localization of the USPION@Gastrin inside the lysosomes. A significant decrease in the Pearson's correlation coefficient was observed after 15 minutes of RMF exposure (0.61 ± 0.3 and 0.70 ± 0.04 in cells exposed or not to RMF). This decrease was more pronounced after 30 minutes (0.46 ± 0.03 vs 0.75 ± 0.05) and 45 minutes (0.31 ± 0.03 vs 0.73 ± 0.06) of RMF application, indicating a decrease of co-localization between USPION@Gastrin and Lysotracker under RMF exposure. The combination of RMF and MNPs therefore results in the lysosome membrane permeabilization, as demonstrated in our previous article [23]. These results shows that lysosome membrane permeabilization is an early event induced by the mechanical forces generated by USPION@Gastrin under RMF. Figure 2c represents the evolution of the fluorescence intensity of the Lysotracker under various conditions. RMF application led to a rapid and significant drop in the Lysotracker fluorescence intensity of the lysosomes containing USPION@Gastrin whereas it does not affect lysosomes devoid of nanoparticles. Indeed, the Lysotracker fluorescence intensity decreased significantly after 5 minutes of RMF application, until it reached a plateau after 15 minutes, displaying an intensity 54.9 % lower than the control cells devoid of nanoparticles and non-exposed to RMF (18.3 ± 8.2 % vs 73.2 ± 4.1 % of the initial value of Lysotraker fluorescence intensity corresponding to 81.7 ± 8.2 % vs 26.8 ± 4.1 % decreases in Lysotraker fluorescence intensity). Of note, the presence of MNPs or RMF exposure slightly decreases the Lysotracker fluorescence intensity by 19.1 % comparatively to control cells (54.1 ± 3.8 % vs 73.2 ± 4.1 % of the initial value of Lysotraker fluorescence intensity corresponding to 45.9 ± 3.8 % vs 26.8 ± 4.1 % decreases in Lysotraker fluorescence intensity), indicating a potential cytotoxic effect just from the accumulation of MNPs in the lysosomes. In absence of MNPs, RMF exposure does not affect the lysosome membrane integrity.

In addition to lysosome permeabilization, we also observed magnetic field-induced MNPs motion (Figure 3), which was quantified using Imaris software. Figure 3a represents the average displacement of lysosomes relative to their starting points during 40 min, given that the 40 mT / 1 Hz RMF was applied from 10 to 30 minutes after the start of the experiment. The average displacement of lysosomes is affected by RMF exposure and significantly increases after 6 minutes of field application ($p<0.001$). Despite the field is switched off at the 30th minute, the lysosomes keep on moving, reaching 10 µm at the end of the experiments, whereas the three other conditions present an average displacement of about 4 µm.

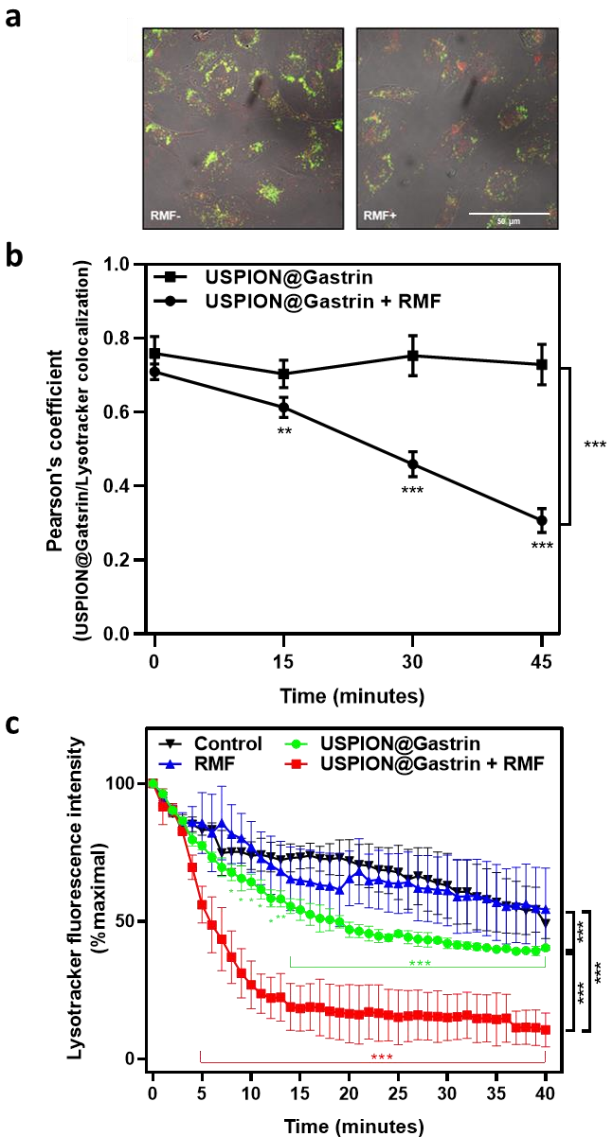

Figure 2. Induction of lysosome permeabilization by MNPs motion under RMF. (a) Confocal images of CAF cells incubated with Lysotracker (green) and USPION@Gastrin (red) and exposed (RMF+) or not (RMF-) to a 40 mT / 1 Hz RMF for 40 minutes. (b) Analysis of colocalization between USPION@Gastrin and Lysotracker labeling of the confocal microscopy images using Pearson's correlation coefficient (ImageJ software). The results are the mean ± SEM of five independent experiments.Statistical analysis performed using ANOVA: under the curve versus t=0, bracket USPION@Gastrin + RMF *versus* USPION@Gastrin. (c) Evolution of the Lysotracker fluorescence intensity in control cells (without USPION@Gastrin and RMF) and in cells treated with RMF or with USPION@Gastrin or with USPION@Gastrin and RMF. The results are the mean ± SEM of three independent experiments. Statistical analysis performed using ANOVA: in color versus t=0, in black between conditions.

Lysosomes are broadly distributed throughout the cytoplasm. Such distribution has been observed in pancreatic CAFs [23]. Although some lysosomes are relatively static, others move bidirectionally along microtubule tracks between the center and the periphery of the cell [24]. We thus analyzed the direction of lysosomes displacement containing or not USPION@Gastrin, relatively to the cell nucleus position during the RMF exposure (Figure 3b). In the presence of USPION@Gastrin, the lysosomes distribution widens with 78% of them getting closer to the cell nucleus (97 of 124 analyzed lysosomes), whereas lysosomes devoid of MNPs weakly and randomly moved around their initial position (supplemental information, Movies M1 and M2). These results showed that RMF application causes a significant displacement of the lysosomes containing MNPs towards the nucleus and the center of the cell.

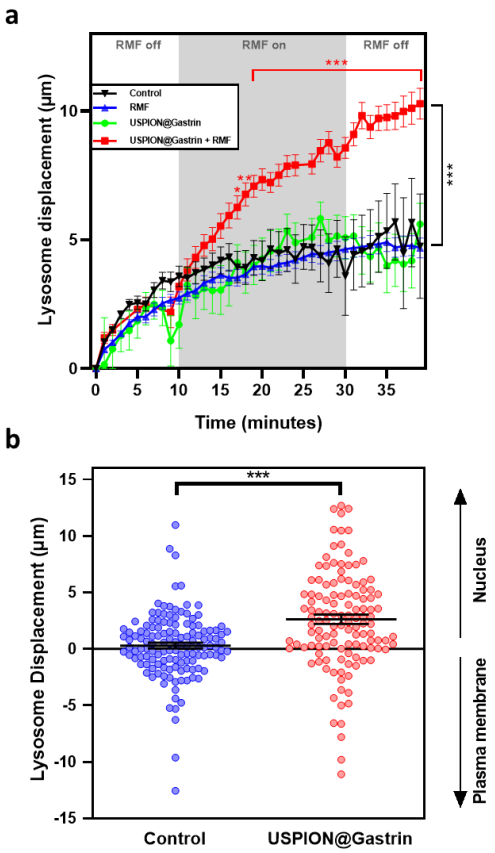

Figure 3. Displacement of lysosomes by MNPs motion under RMF. The cells were exposed or not to a sequence (10 min off / 20 min on / 10 min off) of a 40 mT / 1 Hz RMF in the presence or absence of USPION@Gastrin. (a) Displacement of lysosomes from their starting point in CAF cells. The results are the mean ± SEM of at least three independent experiments (Control: 131, RMF: 169, USPION@Gastrin: 100, USPION@Gastrin + RMF: 132 lysosomes). Statistical analysis performed using ANOVA. (b) Direction of the lysosomes displacement relative to the nucleus after 30 min of RMF exposure in the presence of USPION@Gastrin or not (control). The results are the mean ± SEM of three independent experiments (Control: 133, USPION@Gastrin: 124 lysosomes). Statistical analysis performed using t-test.

Lysosomes movements are orchestrated by motor proteins moving along microtubules [24]. We then investigated whether MNPs motion that induced lysosome displacements also impacted the tubulin microtubules network (Figure 4). Figure 4a represents snapshots of CAF cells devoid of MNPs (RMF) or loaded with USPION@Gastrin (USPION@Gastrin + RMF) at t0 and after 30 min of RMF application. Whereas RMF application did not affect the tubulin filaments and lysosomes integrity of cells devoid of MNPs, it strongly decreases both Lysotracker and TubulinTracker fluorescence intensities in cells loaded with USPION@Gastrin, indicating a significant disruption of tubulin microtubules network (supplemental information, Movies V3 and V4). We analyzed the length and the volume of the filaments constituting the tubulin microtubules cytoskeleton using Imaris software (Figures 4b and 4c). The tubulin microtubules length and volume decreased significantly after 10 minutes of RMF application (t20), displaying a length and a volume 21.9 % and 24.5 % lower than the ones of control cells devoid of nanoparticles and exposed to RMF (78.1 ± 4.0 % vs 96.2 ± 3.7 % of the initial value of microtubules length, 75.5 ± 3.1 % vs 95.4 ± 4.6 % of the initial value of microtubules volume). Longer RMF exposures affected the integrity of the tubulin filaments to a greater extent. Indeed, the microtubules length and volume decreased respectively by 35.9 % and 31 % after 30 minutes of RMF exposure (51.7 ± 4.3 % vs 87.6 ± 5.9 % of the initial value of microtubules length, 50.9 ± 7.3 % vs 81.9 ± 7.4 % of the initial value of microtubules volume), indicating that RMF-induced MNPs motion inside lysosome caused the disruption of tubulin filaments and acted as a microtubule-destabilizing agent. Moreover, this microtubules disorganization constituted an early biological event triggered by MNPs motion.

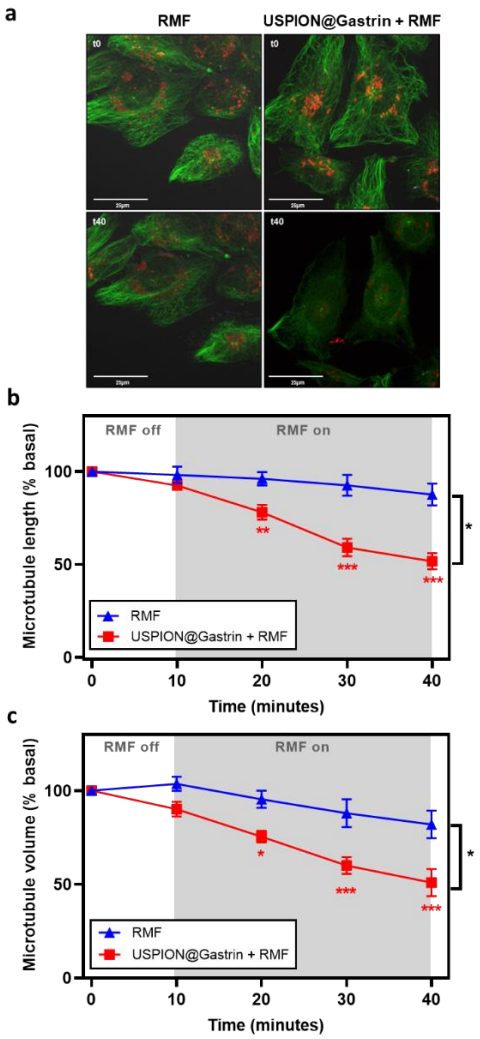

Figure 4. Tubulin microtubules disruption by MNPs motion under RMF. (a) Confocal images of tubulin microtubules. Cells having accumulated (USPION@Gastrin + RMF) or not (RMF) MNPs were exposed to 40 mT/1 Hz RMF from 10 to 40 minutes. Cell lysosomes were stained by Lysotracker (red) and TubulinTracker probe (green). (b) Analysis of tubulin microtubules length using Imaris software. (c) Analysis of tubulin microtubules volume using Imaris software. The results are the mean ± SEM of five independent experiments. Statistical analysis performed using t-test: in red at one time point, in black between curve conditions.

Cytoskeleton disorganization such as microtubule network disruption is known to be associated with the alteration in the cell shape and morphology as well as with the induction of cell death [23]. We thus analyzed the impact of RMF-induced MNPs motion on cell morphology (Figure 5). The observation of the transmission images highlighted a loss of the adhesion surface of the cells containing MNPs and exposed to RMF. Figure 5a depicted a representative image of a CAF cell loaded with USPION@Gastrin and exposed to RMF for 20 minutes (from t=10 to t=30 min). The delineation of the cell perimeter did not present any variation in the cell adhesion surface in absence of RMF exposure (from t=0 to t=10 min, yellow and blue lines respectively). In contrast, the RMF application for 20 minutes led to a loss of the cell adhesion surface (t=30 min, red line), making the cell shrinks. The temporal evolution of the cell adhesion surface was quantified in Figure 5b and showed that the RMF application for 20 minutes decreased significatively the adhesion surface of cell containing USPION@Gastrin by 30.8 ± 2.1 %, without affecting the one of cells devoid of MNPs. Interestingly, the effect of MNPs motion on cell adhesion surface was significant starting from the 7th minute of RMF exposure and characterized by a 12.1 ± 2.5 % decrease in cell adhesion surface. Interestingly, we also observe that some cells totally lose their adhesion property and are detached from the support in response to RMF application (Supplemental information, Movie V5). This result indicates that the loss of cell adhesion surface constituted an early event induced by MNPs motion concomitantly with the lysosome permeabilization and displacement as well as the microtubules network disorganization.

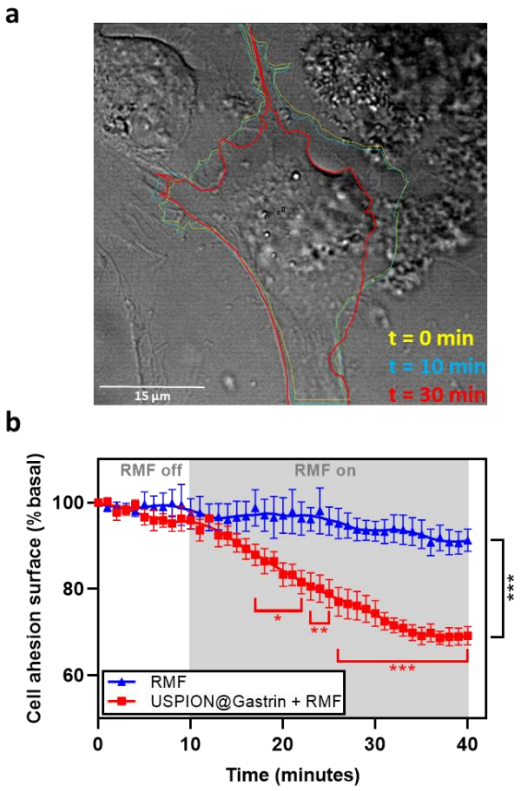

Figure 5. Loss of cell adhesion surface induced by MNPs motion under RMF. (a) Confocal image of a CAF cell incubated with USPION@gastrin non-exposed to RMF (t=0, yellow line) and exposed to a 40 mT / 1 Hz RMF for 20 minutes (from t = 10 to 30 minutes, blue and red lines). (b) Evolution of the cell adhesion surface. The cells containing or not USPION@Gastrin were exposed to 40 mT/1 Hz RMF from 10 to 30 minutes. The results are the mean ± SEM of at least three independent experiments. Statistical analysis performed using t-test: in red at one time point, in black between curve conditions.

While many authors described partial events and usually after treatment, here we go further by observing, in real-time with confocal microscopy, the mechanisms triggered by MNPs motion using a home-made miniaturized electromagnet generating the RMF. One strength of our study is thus that we were able to establish a precise timetable of the events triggered by RMF-induced motion of ultra-small MNPs. We showed that their motion caused concomitantly the lysosome permeabilization and displacements as well as the tubulin microtubules network disorganization and change in cell morphology and adhesion. Moreover, all these events are early induced by MNPs motion since they occurred in the 5 to 10 minutes of RMF exposure.

Regarding the literature, many studies reported about a lysosome permeabilization through heat and/or mechanical damage. Playing an essential role in various programmed cell death pathways, lysosomes are notably involved in the processes of apoptosis [25,26]. The effect of mechanical forces on cell adhesion has been studied by Jeon *et al.* [27]. These authors observed the change in fibroblasts morphology having internalized MNPs (10-120 nm) and exposed to a static magnetic field: their height was reduced, and their adhesion surface increased after treatment. These effects may be due to the movement of internalized and membrane MNPs that are attracted towards the magnet placed below the cell, which forces the cell to lower and stretch, a situation magnetically very different from ours. The impact of a pulsed AC low frequency magnetic field (62 mT/ 50 Hz) treatment on the cell cytoskeleton was studied by Master *et al.* [21]. After accumulation of MNPs of 7-8 nm into lysosomes, a disturbance of the cancer cell cytoskeleton was observed following the magnetic field application. Interestingly, they did not observe lysosome permeabilization after 15 minutes of magnetic field exposure, suggesting that RMF application may be more effective than pulsed AC low frequency magnetic field to induce lysosome disruption. Interestingly, we also showed the migration of the lysosomes toward the center of the cell, a biological effect that has never been reported previously to our knowledge.

We discuss thereafter the mechanisms at the origin of lysosome permeabilization. We previously demonstrated using magnetic simulations that the assembly of 3,000 ultra-small MNPs (6 nm crystalline core) accumulated in lysosomes generate magnetic forces around 3 pN, a value which is well below the tens to hundreds of pN required to disrupt a bilayer membrane [28], suggesting that lysosome permeabilization or rupture induced by USPION@Gastrin torque may involve an alternative mechanism. Mechano-sensitive ion channels can be activated by few pN mechanical forces [29]. Interestingly, mechano-sensitive ion channels such as the Transient Receptor Potential channels TRPML1 and TRPML2 have been identified in endo-lysosomes and interacted with microtubules networks, regulates the endo-lysosomes trafficking, and are involved in cell death through apoptosis or lysosomal pathway when dysregulated [30,31]. The dysregulation of endo-lysosomal TRPML receptors activity induced by MNPs motion under RMF exposure may be involved with the lysosome permeabilization and mobility leading to the disorganization of microtubules network, the change in cell morphology and adhesion, and eventually cell death.

In conclusion, a miniaturized electromagnet allowing real-time analyzes during the RMF application has permitted us to observe different cellular events associated with cell death and induced by MNPs motion located into the lysosomes. In response to the low frequency RMF,

the MNPs generate mechanical forces strong enough to induce the disruption of the lysosome integrity and the leakage of lysosomal content. Concomitantly, the movement of MNPs generate pressure onto the lysosomes attached to the microtubule filaments inducing lysosome mobility, microtubules disruption and cell shrinkage. The dynamic forces generated by MNPs motion under RMF are well below to disrupt directly the bilayer membrane of the lysosomes, but may activate osmo-mechanical sensitive ion channels, such as TRPML, whose activity dysregulation is associated with lysosome permeabilization and motility.

ASSOCIATED CONTENT

Supporting Information

The Supporting Information is available.

AUTHOR INFORMATION

Corresponding Author

*: Correspondance: Véronique Gigoux, INSERM ERL1226, 1 Avenue du Professeur Jean Poulhes, F-31432 Toulouse, France. Email: veronique.gigoux@inserm.fr - Julian Carrey, LPCNO-CNRS UMR5215, 135 avenue de Rangueil, F-31077 Toulouse, France. Email: julian.carrey@insa-toulouse.fr - Laurence Motte, Université Sorbonne Paris Nord, Laboratory for Vascular Translational Science, LVTS, INSERM, UMR 1148, F- 93000 Bobigny, France Email: laurence.motte @sorbonne-paris-nord.fr

Author Contributions

#: These authors contributed equally. S.L., N.H. and P.C. contributed equally to this work. L.M., J.C. and V.G. contributed equally to this work.

Notes

The authors declare no competing financial interest.

ACKNOWLEDGMENT

This research was partly funded by the Instituts thématiques multi-organismes (ITMO) Cancer grant “Domain of Physics, Mathematics or Engineering Sciences” N° 17CP070-000 and the Cancéropôle Grand Sud-Ouest. S.L. is supported by grants from Ligue Nationale Contre le Cancer. We thank Cellular Imaging Facility Rangueil and Flow Cytometry platform of I2MC/INSERM for the excellent technical support.

The authors want to overall remark the clear contribution of the French government in destroying the research and university of France and the future of a complete generation. #StopLPPR

REFERENCES

1. Pankhurst, Q. A., Connolly, J., Jones, S. K. & Dobson, J. P. Applications of magnetic nanoparticles in biomedicine. vol. 36 167–181 (2003).
2. Cheng, Y. Y., Morshed, R. A., Auffinger, B., Tobias, A. L. & Lesniak, M. S. Multifunctional nanoparticles for brain tumor imaging and therapy. vol. 66 42–57 (2014).
3. Stephen, Z. R., Kievit, F. M. & Zhang, M. Magnetite nanoparticles for medical MR imaging. *Mater. Today* **14**, 330–338 (2011).
4. Jin, R., Lin, B., Li, D. & Ai, H. Superparamagnetic iron oxide nanoparticles for MR imaging and therapy: design considerations and clinical applications. *Curr. Opin. Pharmacol.* **18**, 18–27 (2014).
5. Arruebo, M., Fernández-Pacheco, R., Ibarra, M. R. & Santamaría, J. Magnetic nanoparticles for drug delivery. *Nano Today* **2**, 22–32 (2007).
6. Mody, V. V. *et al.* Magnetic nanoparticle drug delivery systems for targeting tumor. *Appl. Nanosci.* **4**, 385–392 (2014).
7. Sun, C., Lee, J. S. H. H. & Zhang, M. Magnetic nanoparticles in MR imaging and drug delivery. vol. 60 1252–1265 (2008).
8. Sanchez, C. *et al.* Targeting a G-protein-coupled receptor overexpressed in endocrine tumors by magnetic nanoparticles to induce cell death. *ACS Nano* **8**, 1350–1363 (2014).
9. Kafrouni, L. & Savadogo, O. Recent progress on magnetic nanoparticles for magnetic hyperthermia. *Prog. Biomater.* **5**, 147–160 (2016).
10. Dutz, S. & Hergt, R. Magnetic particle hyperthermia – a promising tumour therapy? *Nanotechnology* **25**, 1–28 (2014).
11. Mannix, R. J. *et al.* Nanomagnetic actuation of receptor-mediated signal transduction. *Nat Nanotechnol* **3**, 36–40 (2008).
12. Hughes, S., McBain, S., Dobson, J. P. & Haj, A. J. El. Selective activation of mechanosensitive ion channels using magnetic particles. *J. R. Soc., Interface* **5**, 855–863 (2008).
13. Fung, A. O., Kapadia, V., Pierstorff, E., Ho, D. & Chen, Y. Induction of cell death by magnetic actuation of nickel nanowires internalized by fibroblasts. **112**, 15085–15088 (2008).
14. Goiriena-Goikoetxea, M. *et al.* Disk-shaped magnetic particles for cancer therapy. *Applied Physics Reviews* vol. 7 11306 (2020).
15. Chen, M. *et al.* Remote Control of Mechanical Forces via Mitochondrial-Targeted Magnetic Nanospinners for Efficient Cancer Treatment. *Small* **16**, 1905424 (2020).
16. Maniotis, N. *et al.* Magneto-mechanical action of multimodal field configurations on magnetic nanoparticle environments. *J. Magn. Magn. Mater.* **470**, 6–11 (2019).
17. Carrey, J. & Hallali, N. Torque undergone by assemblies of single-domain magnetic nanoparticles submitted to a rotating magnetic field. *Phys. Rev. B* **94**, (2016).
18. Zhang, E. M. *et al.* Dynamic Magnetic Fields Remote-Control Apoptosis via Nanoparticle Rotation. *ACS Nano* **8**, 3192–3201 (2014).
19. Shen, Y. *et al.* Elongated Nanoparticle Aggregates in Cancer Cells for Mechanical Destruction with Low Frequency Rotating Magnetic Field.

Theranostics **7**, 1735–1748 (2017).
20. Lunov, O. *et al.* Remote actuation of apoptosis in liver cancer cells via magneto-mechanical modulation of iron oxide nanoparticles. *Cancers (Basel).* **11**, 1873 (2019).
21. Master, A. M. *et al.* Remote Actuation of Magnetic Nanoparticles For Cancer Cell Selective Treatment Through Cytoskeletal Disruption. *Sci Rep* **6**, 33560 (2016).
22. Lopez, S. *et al.* Magneto-mechanical destruction of cancer-associated fibroblasts using ultra-small iron oxide nanoparticles and low frequency rotating magnetic fields. *NANOSCALE Adv.* **4**, 421-436 *(2022).* doi:10.1039/d1na00474c.
23. S, L. Magneto-mechanical destruction of cancer-associated fibroblasts using ultra-small superparamagnetic iron oxide nanopar-ticles and low frequency magnetic fields. *Nanoscale Adv.* **In press**, DOI: 10.1039/D1NA00474C. (2021).
24. Pu, J., Guardia, C. M., Keren-Kaplan, T. & Bonifacino, J. S. Mechanisms and functions of lysosome positioning. *J. Cell Sci.* **129**, 4329–4339 (2016).
25. Villamil Giraldo, A. M., Appelqvist, H., Ederth, T. & Ollinger, K. Lysosomotropic agents: impact on lysosomal membrane permeabilization and cell death. *Biochem Soc Trans* **42**, 1460–1464 (2014).
26. Kavčič, N., Pegan, K. & Turk, B. Lysosomes in programmed cell death pathways: from initiators to amplifiers. *Biological Chemistry* vol. 398 289–301 (2017).
27. Jeon, S. *et al.* Surface functionalized magnetic nanoparticles shift cell behavior with on/off magnetic fields. *J. Cell. Physiol.* **233**, 1168–1178 (2018).
28. Golovin, Y. I. *et al.* Towards nanomedicines of the future: Remote magneto-mechanical actuation of nanomedicines by alternating magnetic fields. *J. Control. Release* **219**, 43–60 (2015).
29. Li, X. *et al.* A molecular mechanism to regulate lysosome motility for lysosome positioning and tubulation. *Nat. Cell Biol.* **18**, 404–417 (2016).
30. Colletti, G. A. *et al.* Loss of lysosomal ion channel transient receptor potential channel mucolipin-1 (TRPML1) leads to cathepsin B-dependent apoptosis. *J Biol Chem* **287**, 8082–8091 (2012).
31. Morelli, M. B. *et al.* Overexpression of transient receptor potential mucolipin-2 ion channels in gliomas: role in tumor growth and progression. *Oncotarget* **7**, 43654–43668 (2016).